Meteoritics & Planetary Science 39, Nr 3, 453–466 (2004)
Abstract available online at http://meteoritics.org

Production rates and proton-induced production cross sections of ^{129}I from Te and Ba: An attempt to model the ^{129}I production in stony meteoroids and ^{129}I in a Knyahinya sample

C. SCHNABEL,[1, 2, 5, 8*] I. LEYA,[1, 4] M. GLORIS,[1] R. MICHEL,[1] J. M. LOPEZ-GUTIÉRREZ,[2, 7] U. KRÄHENBÜHL,[5] U. HERPERS,[6] J. KUHNHENN,[6] and H. A. SYNAL[3]

[1]Zentrum für Strahlenschutz und Radioökologie (ZSR), Universität Hannover, Am Kleinen Felde 30, D-30167 Hannover, Germany
[2]Institut für Teilchenphysik, ETH Hönggerberg, CH-8093 Zürich, Switzerland
[3]Paul Scherrer Institut, c/o Institut für Teilchenphysik, ETH Hönggerberg, CH-8093 Zürich, Switzerland
[4]Institut für Isotopengeologie, ETH Zürich, Sonneggstrasse 5, CH-8092 Zürich, Switzerland
[5]Departement für Chemie und Biochemie, Universität Bern, Freiestrasse 3, CH-3012 Bern, Switzerland
[6]Abteilung Nuklearchemie, Universität zu Köln, D-50674 Köln, Germany
[7]Departemento de Física Aplicada I, Escuela Universitaria Politécnica, Universidad de Sevilla, E-41011 Sevilla, Spain
[8]Scottish Universities Environmental Research Center, Scottish Enterprise Technology Park, East Kilbride G75 0QF, UK
*Corresponding author. E-mail: c.schnabel@suerc.gla.ac.uk

(Received 02 April 2002; revision accepted 17 January 2004)

Abstract–Proton-induced production cross sections of ^{129}I from Te and Ba are presented. Earlier assumptions that Te is the most important target element in meteoroids are confirmed. Based on this data set and the experimental production rates of ^{129}I from thick-target experiments, the production of ^{129}I in stony meteoroids is modeled using a GCR flux density of 4.06 cm^{-2} s^{-1}. The results of this modeling must be considered preliminary because the contribution from neutron capture on ^{128}Te needs further investigation. We obtained modeled production rates that agree with experimental results for samples from two medium-sized meteorites (Abee and Knyahinya). However, we find that this model does not describe ^{41}Ca in lunar rocks well and seems to overestimate ^{129}I production in larger bodies, such as Allende. We present elemental production rates from Te and Ba based on our modeling as well as for a model that describes neutron capture products. For ^{129}I analysis of Knyahinya, a novel method to separate Te and analysis using ICP-MS was used, enabling the use of experimental elemental concentrations obtained from the same meteorite to calculate ^{129}I production.

INTRODUCTION

Iodine-129 is a nuclide of interest for studies of the irradiation history of extraterrestrial material because its half-life of 1.57×10^7 yr falls into the gap between those of ^{53}Mn (3.7×10^6 yr) and ^{40}K (1.28×10^9 yr). Consequently, ^{129}I can be employed to check the constancy of the galactic cosmic ray (GCR) flux on longer time scales than when using ^{53}Mn or ^{10}Be ($T_{1/2} = 1.5 \times 10^6$ yr). The main sources of ^{129}I production in extraterrestrial material are reactions of neutrons and protons on Te. Besides Te, Ba has also been suggested as a main target element for ^{129}I production in meteoroids. Therefore, we determined the proton-induced production cross sections and production rates of ^{129}I from Te as well as from Ba. In addition, we analyzed ^{129}I as well as Te and Ba concentrations in Knyahinya and the two target elements for ^{129}I production in Abee.

A first determination of ^{129}I in two stony meteorites reported by Elmore et al. (1980) was followed by ^{129}I determination in three stony meteorites and a lunar rock by Nishiizumi et al. (1983). Some years later, Nishiizumi et al. (1985) reported on ^{129}I in the troilite phase of two iron meteorites, and then in a Ba-rich and Te-poor lunar core (Nishiizumi et al. 1989). Further, Nishiizumi et al. (1993) measured ^{129}I in two samples of Fayetteville. Their results, combined with fission track data and noble gas data, indicate a two-stage irradiation of that meteorite. For all meteorite samples, Te was assumed to be the only target element for ^{129}I production so that ^{129}I production rates were calculated based on the Te content of the meteorite and reported as atom ^{129}I min^{-1} × (kg Te)$^{-1}$.

Up to now, only preliminary data for proton-induced production cross sections and production rates of ^{129}I have been published (Schnabel et al. 1997). We have also reported a

production cross section for 14.7 MeV neutrons on Te (Schnabel et al. 2000). Because of the lack of production cross section and thick-target production rate data, the cosmogenic production of ^{129}I in meteoroids from Te and Ba could not be modeled previously. Moreover, no ^{129}I analyses have been reported yet from samples of known shielding depth from meteorites of well-known exposure history and geometry, for which Te and Ba concentrations have been analyzed.

EXPERIMENTAL PROCEDURES

Irradiation Experiments and Flux Density Determinations

In the compact cyclotron CV28 at the Institut für Nuklearchemie, Forschungszentrum Jülich, thin electrolytically-prepared Te samples on titanium foils (10 μm) were irradiated with 19.9 MeV protons (energy of the incident beam) in a stacked foil. Copper foils (25 μm) were used as flux monitors using the reactions Cu(p, xn)^{63}Zn and Cu(p, xn)^{62}Zn and cross sections given by Tarkanyi et al. (2001). For the given energy range, these cross sections are similar to those published by Takacs et al. (2002). Both reactions were also used to determine the exact energy of the incident beam by applying the technique published by Piel et al. (1992).

Proton irradiations of high-purity Cu_2Te samples for the determination of production cross sections were performed at energies from 280 MeV to 2600 MeV (energy of the incident beam) at the Laboratoire National Saturne, Saclay (France) and at 136 MeV to 178 MeV (incident energy) at the T. Svedborg Laboratory, University of Uppsala (Sweden). Proton fluences between 6.56×10^{13} and 2.31×10^{15} cm^{-2} were applied. For these experiments, the proton fluxes were determined via the monitor reaction ^{27}Al(p, 3p3n)^{22}Na, by measuring the ^{22}Na activity in Al foils, and by using the evaluated cross sections of Tobailem et al. (1981) and the data set given by Steyn et al. (1990).

For the determination of production rates of ^{129}I, samples of high-purity Te powder and Ba-glass (Schott, Mainz; Chemical composition in wt%: Ba 40, O 35.7, Si 16.2, B 4.4, Al 3.0) were irradiated isotropically with 1600 MeV protons in cores of artificial meteoroids made of gabbro and iron, respectively. The radii of the irradiated bodies were 25 cm for gabbro and 10 cm for iron (99% purity). The purpose of the gabbro and the iron was to produce secondary particles (especially neutrons) so that the irradiation of a stony meteoroid and an iron meteoroid in space were simulated, respectively. Detailed descriptions of these experiments have been published elsewhere (Leya et al. 2000a).

Radiochemical Procedures for the Irradiated Samples

The radiochemical procedure that was applied depended on the chemical substance to be irradiated. In the case of pure Te, the procedure published by Nishiizumi et al. (1983) for the determination of ^{129}I in stony meteorites was applied in a modified form, as published by Schnabel et al. (2000). Briefly, this procedure included alkaline leaching, isotopic equilibration as iodide, and purification steps including liquid-liquid extractions. For the Ba-glass samples, the same procedure was applied because this material is also soluble in alkaline melts. In this case, typical amounts were 0.2–0.6 g Ba-glass, 1 to 4 g NaOH, and approximately 0.2–0.5 ml water. In the case of copper-(I)-telluride (Cu_2Te), the procedure used for Te and Ba-glass had to be modified further. This is because copper (II), formed from the disproportionation of copper (I) to copper (II) and copper metal, can react with iodide in aqueous solutions, resulting in the production of gaseous iodine and copper-(I)-iodide. Thus, loss of the iodine carrier before isotopic equilibration will occur unless this reaction is prevented. This disequilibrium would lead to measuring an incorrect isotopic ratio of the sample. Moreover, copper-(I)-iodide is insoluble, resulting again in iodine loss before isotopic equilibration. The addition of more sodium thiosulfate than stochiometrically required prevents both reactions because it forms strong complexes with copper (I), resulting in the dissolution of any precipitated copper-(I)-iodide, and also because thiosulfate reduces any molecular iodine formed to iodide. Apart from the addition of excess of thiosulfate, the procedure follows the one used for Te and Ba-glass.

For all materials, the radiochemical procedure was carried out for at least six half-lives of ^{129m}Te ($T_{1/2}$ = 33.6 d), i.e., seven months after the end of the irradiation, to make sure that all precursor nuclides of ^{129}I have decayed to the nuclide of interest. As a quality control measure, for all irradiated substances, at least two aliquots of an irradiated sample were processed separately for at least three samples. The results of these tests will be discussed below.

Sample and Radiochemical Procedure for the Meteorite Knyahinya

More than 20 g of a sample of Knyahinya, Kny ZH (Graf 1988), were kindly provided by R. Wieler, ETH Zürich. Based on the ^{22}Ne/^{21}Ne ratio of 1.12 (Graf 1988), which was confirmed by the model presented by Leya et al. (2000b), the piece came from 7.5–10 cm deep in a body with a 45 cm preatmospheric radius.

20.3 g of Knyahinya was crushed and sieved, resulting in material of <150 μm grain size. No substantial amount of coarse magnetic fraction was observed. 2.82 mg iodide prepared from Woodward iodine (Woodward Iodine Corp., Woodward, Oklahoma) was added as a carrier between layers of the meteorite powder in a nickel crucible. This layered structure was chosen to speed up the mixing of the carrier with the sample. Together with 25 g NaOH and 5 g water, the mixture was treated in the same way as the Te samples described by Schnabel et al. (2000).

Te and Ba analysis of Meteorite Samples

Because of the volatility of Te, techniques that are unaffected by partial loss of the element of interest during the post-irradiation chemical separation, such as radiochemical neutron activation analysis, normally have been applied to determine the concentration of this element in meteorites (e.g., Krähenbühl et al. 1973; Binz et al. 1974; Walsh and Lipschutz 1982). Because access to research reactors has become more difficult, we took advantage of the sensitivity of ICP-MS to determine Te concentrations after we had proven that the chemical procedure used did not give rise to significant losses of this element.

A 1.2 g sample of Knyahinya was crushed and sieved using a 150 μm sieve. A coarse magnetic fraction of 42 mg remained. Three samples of 100 mg each were taken from the fine fraction. The samples were dissolved in Teflon pressure bombs in a mixture of 3 ml 65% HNO_3, 2 ml 30% H_2O_2, 1 ml 40% HF, and 2 mg MgO. All reagents were of suprapure quality. The resulting solutions were diluted to 100 ml and measured on a double-focusing sector field ICP-MS (Finnigan Element 2) for Te and Ba relative to standard solutions. The blank correction amounted to less than 5% of the content of the investigated elements. In earlier experiments, it had been demonstrated that, with this chemical procedure, no significant loss of Te occurred (<10%). For Abee, about 32 mg were processed in the same way as described for the Knyahinya samples above.

AMS Measurement

The ^{129}I measurements were performed at the PSI/ETH 6 MV tandem accelerator mass spectrometer (AMS). The AMS was operated at a terminal voltage of 4.7 MV. The 5^+ charge state was selected after the gas stripper. To improve the mass separation of ^{129}I from Te and stable iodine, a time-of-flight spectrometer developed by Lopez-Gutierrez et al. (2000) was used.

The ^{129}I content of the samples was measured by comparison with standards prepared by diluting the NBS standard reference material 4949B to a nominal $^{129}I/^{127}I$ ratio of 4.74×10^{-11}. Measured $^{129}I/^{127}I$ ratios for blanks from unirradiated Te or Cu_2Te, which were processed in the same way as the samples, were $1–2 \times 10^{-13}$. The samples produced isotopic ratios of about 10^{-10} to 10^{-9}. For the Ba-glass samples and the Knyahinya sample, the isotopic ratios were as low as 4×10^{-12} to 1×10^{-11} so that a blank correction was necessary for these samples. Details of the measurement technique are given by Lopez-Gutierrez et al. (2000) and Synal et al. (1997).

EXPERIMENTAL RESULTS

Cross section and production rate data are given in Tables 1–3. Uncertainties include the standard uncertainty of the determination of the flux density and either the average standard uncertainty of the AMS measurements or the standard deviation of the mean of the AMS measurements of different aliquots, whichever is higher. The same criterion applies to the production rate data from Ba that is only shown graphically in Figs. 4a and 4b.

Production Cross Sections From Te

Our measured cross sections for the proton-induced production of ^{129}I from Te are presented in Table 1 and shown in Fig. 1. The figure also depicts the adjusted excitation function of ^{129}I from Te used to model the ^{129}I production rates in meteoroids in the energy range up to 50 MeV, as discussed below.

Below 20 MeV, the ^{130}Te(p, 2n)^{129}I reaction is by far the dominant production channel of ^{129}I. Consequently, our results can be compared to those obtained by the Jülich group for (p, 2n) reactions on other Te isotopes (Hohn et al. 1998a, 1998b, 2001; Scholten et al. 1995).

The experimental data exhibit the expected evaporation peak from the ^{130}Te(p, 2n)^{129}I reaction to be between 10 and 20 MeV. According to Hybrid-Model calculations, no other maxima of the excitation function are expected from the other reaction channels, i.e., ^{130}Te(p, pn β^-)^{129}I and ^{130}Te(p, 2p $2\beta^-$)^{129}I. Consequently, the local maximum at 95 MeV

Table 1. Cross sections (σ) for the proton-induced production of ^{129}I from Te.

E (MeV)	σ (mb)	Irradiated material
13.09 ± 0.18	403 ± 32	Te
14.51 ± 0.18	478 ± 38	Te
15.90 ± 0.18	454 ± 63	Te
17.10 ± 0.18	506 ± 40	Te
19.43 ± 0.17	439 ± 35	Te
29.1 ± 2.9	208 ± 23	Cu_2Te
36.4 ± 0.9	141 ± 11	Te
61.4	54.1 ± 2.9	Cu_2Te
62.5	81.2 ± 4.8	Cu_2Te
95.1	90.7 ± 7.4	Cu_2Te
128.3	35.3 ± 1.8	Cu_2Te
221.4	32.8 ± 1.2	Cu_2Te
224.7	29.1 ± 1.0	Te
236	31.6 ± 5.3	Cu_2Te
271	30.5 ± 5.3	Cu_2Te
350	29.2 ± 2.1	Cu_2Te
567	34.5 ± 9.1	Cu_2Te
769	32.0 ± 4.2	Cu_2Te
977	35.8 ± 1.2	Cu_2Te
1180	23.2 ± 3.0	Cu_2Te
1378	37.3 ± 2.6	Cu_2Te
1580	25.4 ± 4.3	Cu_2Te
2572	39.8 ± 0.6	Cu_2Te
2575	39.9 ± 1.0	Te
2580	27.6 ± 8.5	Cu_2Te

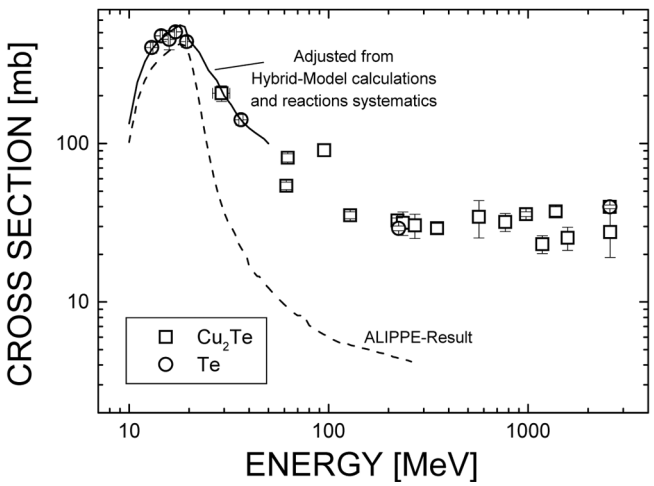

Fig. 1. Excitation function for the p-induced production of ^{129}I in Te experimental and theoretical data.

does not reflect an evaporation peak of a different reaction channel but, apparently, is due to difficulties with the chemical separation of Cu_2Te that occurred in a few cases and are discussed in detail below. Unexpected structures in the excitation function at higher energies were also found in the reaction Te(p, X)^{129m}Te (Gloris 1997, personal communication) and have been attributed to difficulties with the flux density determination. However, the resulting uncertainties in the production cross sections above 100 MeV should not give rise to a large uncertainty in the modeling of the production of ^{129}I in meteorites because the major contributions to that production are from neutrons and protons below 50 MeV.

Of all irradiated Cu_2Te samples, at least two aliquots were processed and measured separately because of the possibility of losing some ^{127}I carrier before isotopic equilibration, as discussed above. For most samples, similar amounts were processed in the respective aliquots. For nine samples for which two aliquots each were processed, the average standard deviation of the means was 4.0%, while the average standard variation of the respective AMS measurements of the aliquots was 4.8%. This demonstrates that, for these samples, no systematic error should be attributed to the chemical separation technique. However, for a few samples, the scatter of the results for the cross sections of the individual aliquots was quite high, leading to relative standard deviations of the mean value (weighted by the masses of processed Cu_2Te) of as much as 20%. This was the case for the samples irradiated at 567 and 2580 MeV. These samples were among the first samples processed, and in these cases, the aliquots did not contain similar masses of irradiated Cu_2Te resulting in a high weight for one of the aliquots during the calculation of the weighted average. In conclusion, the chemical procedure chosen for Cu_2Te can be considered reliable when it is used for at least two aliquots of similar masses.

Table 2. Production rates of ^{129}I from Te for protons with an incident energy of 1600 MeV in gabbro and in iron. Data are normalized to a proton flux density of 1 cm^{-2} s^{-1}.

Irradiated material	Depth (cm)	Production rate (atom min^{-1} [kg Te^{-1}])
Gabbro	3.5	44.4 ± 3.5
Gabbro	8.5	59.6 ± 5.1
Gabbro	13.5	65.0 ± 5.1
Gabbro	18.5	66.8 ± 7.0
Iron	2.01	54.1 ± 5.8
Iron	4.80	60.1 ± 7.4
Iron	7.21	58.9 ± 6.4

Production Rates of ^{129}I From Te

The production rates of ^{129}I from Te obtained from the isotropic irradiations of a gabbro and an iron sphere with 1600 MeV protons are given in Table 2 and shown in Figs. 2a and 2b. All production rates are normalized to a proton flux density of 1 cm^{-2} s^{-1}. To convert these production rates from the simulation experiment to production rates of ^{129}I from Te in real meteoroids, these production rates first have to be recalculated for the real GCR spectrum, which has an average energy above 2000 MeV. These converted production rates, as a function of depth and size, which are still normalized to a flux density of 1 cm^{-2} s^{-1}, can then be multiplied by a factor of 4.06 to obtain the production rates for spallogenic reactions in real meteoroids. This procedure is described in detail in Leya et al. (2000b).

In Figs. 2a and 2b, we also show the results of model calculations for the contributions of neutron capture on ^{128}Te and of reactions induced by primary and secondary protons, as well as the contributions of fast secondary neutrons to the production of ^{129}I. The Monte Carlo codes used to derive the depth-dependent particle spectra inside the irradiated objects are cited in Leya et al. (2000b). From the measured total production rates, the calculated contributions from protons and thermal neutrons were subtracted. From these resulting production rates, which are only due to fast secondary neutrons, the neutron excitation function was derived from an energy dependent least-squares adjustment procedure (e.g., Leya et al. 2000a). To calculate the proton induced component, we rely on our measured cross sections. Between 10 and 50 MeV, the results of the model calculations, based on the Hybrid-Model of pre-equilibrium reactions (Blann 1972) using the ALICE-IPPE code (Shubin et al. 1995) and adjusted to our data, were used to allow for a proper interpolation between our experimental cross sections. Since this code did not calculate any cross sections below 10 MeV, cross sections were interpolated between the calculated reaction threshold and the adjusted ALICE-IPPE result at 10 MeV. Above 50 MeV, we relied on our measured cross sections without any smoothing. The thermal neutron capture component was calculated using the cross sections from the

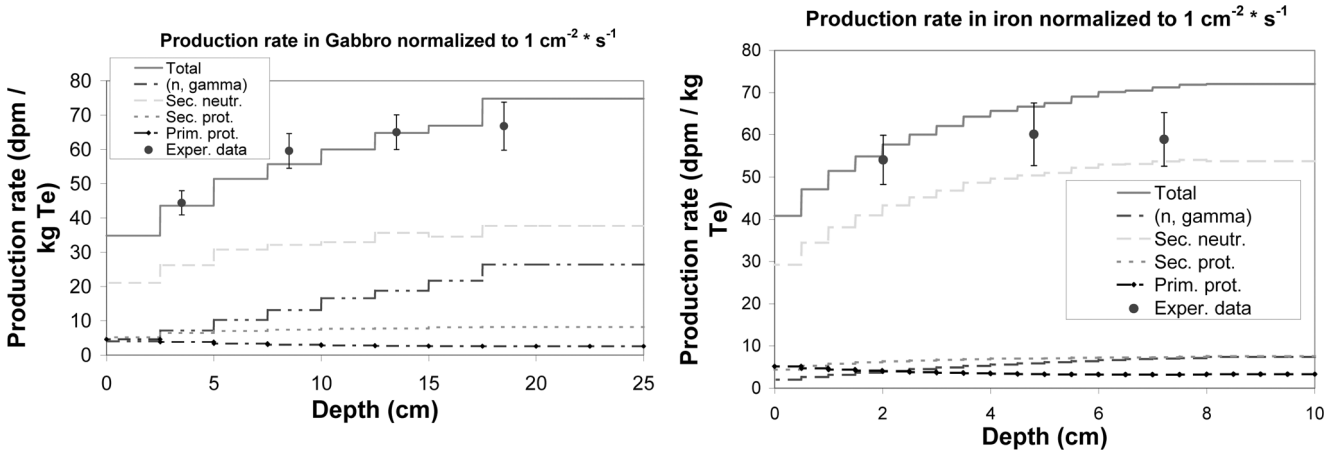

Fig. 2. a and b) Experimental and modeled production rates of ^{129}I from Te for protons with an incident energy of 1600 MeV in gabbro and in iron, respectively. The data are normalized to a proton flux density of 1 cm^{-2} s^{-1}.

JEF-2 database (JEF-2.2 2000). Besides the production rates from the two irradiation experiments and an estimated function for the neutron excitation function, we also included the weighted mean of our experimental neutron-induced cross section at 14.7 MeV (Schnabel et al. 2000) in the least-squares adjustment procedure. The estimated neutron excitation function was then calculated again using the ALICE-IPPE code (Shubin et al. 1995). This excitation function was adjusted in such a way that it agreed with the measured 14.7 MeV cross section within 1σ of the experimental data point. Moreover, the adjustment was only carried out between the threshold and 20 MeV.

For the gabbro sphere, the calculated production rate profile is slightly steeper than the slope given by the experimental data points. This may be due to a slight overestimation of the (n, γ) contribution.

For six of the seven Te samples, two aliquots were processed and measured separately. The average standard deviation of the means of the two aliquots was 9.2%, while the mean standard deviation of the AMS measurements of the respective single samples amounted to 11.2%. From this, the conclusion can be reached that the radiochemical procedure used is reliable for irradiated Te samples. This conclusion had also been reached by Schnabel et al. (2000).

Production Cross Sections of ^{129}I From Ba

We also determined proton-induced production cross sections from Ba for two reasons. First, Nishiizumi et al. (1989) calculated that Ba should dominate ^{129}I production in Ba-rich and Te-poor lunar samples. Second, for H chondrites, Ba is approximately 16 times more abundant than Te (average of all petrographic types; Wasson and Kallemeyn 1988), leading to the expectation that ^{129}I from Ba should not be negligible especially for the higher petrographic types of this meteorite class, where Te contents are lower.

Our experimental cross sections for the proton-induced production of ^{129}I from Ba are summarized in Table 3 and also shown together with cross sections obtained from nuclear model codes in Fig. 3. The latter were calculated again using the ALICE-IPPE code (Shubin et al. 1995). For the calculated data, the total excitation function as well as the individual contributions from ^{138}Ba, ^{137}Ba, and ^{136}Ba are shown in Fig. 3. It is important to emphasize that the Hybrid-Model calculations are not adjusted to the experimental data. The good agreement between the calculated data and the measurements at energies of about 100–200 MeV shows that the present version of the Hybrid-Model is able to accurately calculate proton-induced cross sections for heavy target elements at intermediate energies. The systematic drop-off of the Hybrid-Model calculations above 200 MeV, which is not seen in the experimental data, is due to the dominance of spallation reactions in that energy range, which are not included in the Hybrid-Model. This effect does not influence the calculation of the ^{129}I production rates from Ba because, for modeling the ^{129}I production rates in meteoroids, the ALICE-IPPE results were only used below 90 MeV, where no experimental cross sections are available. For higher energies, we rely on our experimental cross sections for modeling.

For quality control, two aliquots of four Ba-glass samples from the 600 MeV meteoroid simulation experiment were chemically processed and measured for ^{129}I separately, although the results are not shown in the figure. The average standard deviation of the AMS measurements of the single samples amounted to 5.8%, while the average standard deviation of the means of the ^{129}I concentrations of the two aliquots was 4.8%. Again, the radiochemical procedure chosen for Ba-glass gives reproducible results. The lack of local maxima and minima of the experimental data between 100 and 200 MeV, which are not expected from nuclear reaction mechanisms, also gives confidence in the reliability of the radiochemical procedure used.

Table 3. Cross sections for the reaction Ba(p, 4p, xn)^{129}I

E (MeV)	σ (mb)
92.3 ± 3.8	0.101 ± 0.012
108 ± 4	0.237 ± 0.022
117 ± 4	0.296 ± 0.027
128 ± 3	0.314 ± 0.029
138 ± 3	0.416 ± 0.061
151 ± 3	0.461 ± 0.059
160 ± 3	0.516 ± 0.052
169 ± 3	0.586 ± 0.056
207 ± 3	1.07 ± 0.05
600	3.24 ± 0.14
1180 ± 2	2.81 ± 0.09
1580 ± 2	2.34 ± 0.09
2580 ± 2	2.75 ± 0.14

Production Rates of ^{129}I From Ba

Our experimental data for the normalized production rates of ^{129}I from Ba for the 1600 MeV thick target experiments are shown graphically in Figs. 4a and 4b. The depth profiles of ^{129}I from Ba are plotted for both the iron and the gabbro sphere, respectively. As expected from the comparison of the proton-induced production cross sections of ^{129}I from Te and Ba, the elemental production rates from Ba are about a factor of 50 lower than those from Te. Both profiles are flatter than the profiles obtained for the production from Te. This difference is partly due to the fact that the relative contribution of neutrons to the production of ^{129}I is smaller because neither neutron capture nor a reaction such as (n, 2n) can produce ^{129}I from Ba. In addition, the relative mass difference between product and target isotope is much larger for Ba than Te, as the dominant isotope is ^{138}Ba. Therefore, the overall ^{129}I production rates are higher for Te than for Ba, with Te showing a much stronger depth dependency than Ba.

The relative standard deviations for some Ba samples in Figs. 4a and 4b are much larger than those for the production rates from Te. The standard deviation in these cases reflects the standard deviation of two independent AMS measurements of the same sample.

EXPERIMENTAL RESULTS FOR KNYAHINYA AND ABEE

Results of the ^{129}I Analysis of Knyahinya

The AgI sample resulting from the radiochemical processing of the 20.3 g Knyahinya sample was measured four times during two different experimental runs. The blank-corrected results for the measured isotopic ratios and the derived ^{129}I atom concentrations are shown in Table 4. The production rates of ^{129}I, which were calculated using an exposure age of 39.4 Myr (Leya et al. 2000b), are also presented in Table 4. This age is in excellent agreement with the ^{81}Kr-Kr age of 39.5 Myr obtained by Lavielle et al. (1997). The blank correction of the ^{129}I content amounted to ~3%. The results in Table 4 are slightly lower than the preliminary data presented by Schnabel et al. (2001) because the measurements are more complete. The production rate obtained for this sample, from 7.5–10.0 cm depth, is compared to the results of our modeling calculations below.

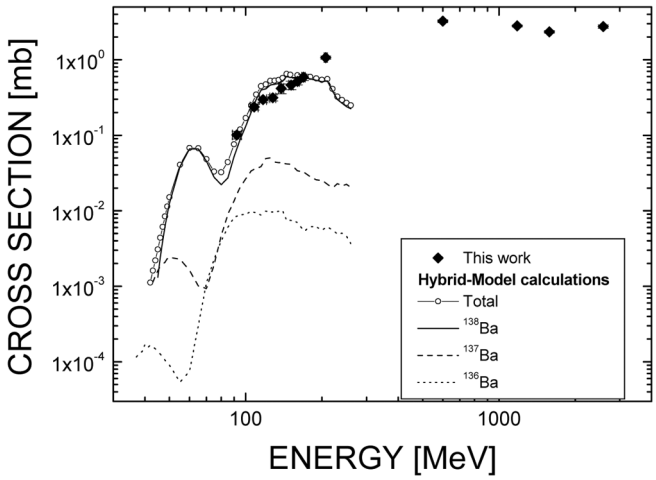

Fig. 3. Experimental and theoretical excitation function for the p-induced production of ^{129}I in Ba.

Results of Te and Ba Analysis for Knyahinya and Abee

The Te and Ba contents of three silicate and one magnetic phase sample of Knyahinya, obtained using the chemical procedure discussed, are shown in Table 5a and compared to literature data for L chondrites in Table 5b.

Our Te concentrations are only slightly higher than the one given by Wasson and Kallemeyn (1988) for L chondrites, but greater than the concentration determined for Knyahinya by Walsh and Lipschutz (1982). However, the Te concentration of 526 µg/kg for Knyahinya bulk (L5) presented here is comparable to the same authors' result for Tadjera (L5) of 507 µg Te/kg. We believe that these are the first Te concentrations in meteorites that were obtained using a technique other than neutron activation analysis.

For Ba, we obtained good reproducibility for the three different silicate aliquots and for low blank values. However, our result clearly exceeds the concentration of Wasson and Kallemeyn (1988) for bulk L chondrites, but the magnetic phase is comparable to the bulk value given by Wasson and Kallemeyn (1988).

For the Abee sample, we obtained 2.40 ± 0.24 mg Te/kg bulk and 3.15 ± 0.32 mg Ba/kg bulk. The Te concentration we obtained for Abee is in very good agreement with the 2.41 mg Te/kg determined by Hertogen et al. (1983) and agrees within 1σ with the concentration of 2.23 mg Te/kg compiled by Wasson and Kallemeyn (1988) for EH chondrites. Additionally, the Ba concentration measured in Abee agrees within 2σ with the concentration of 2.6 mg Ba/

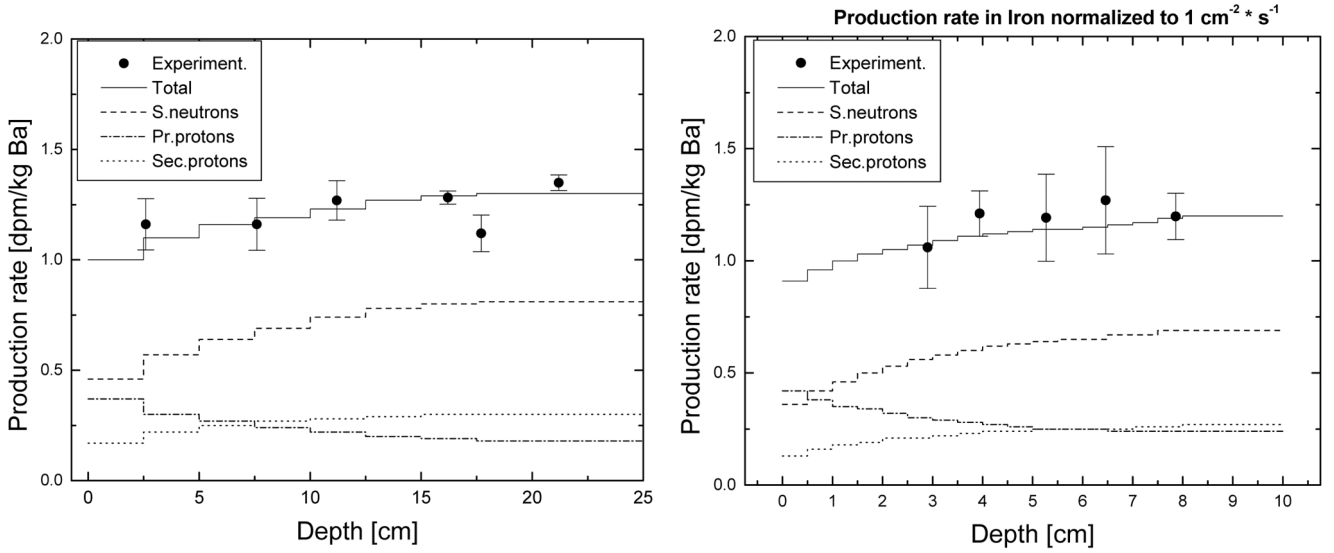

Fig. 4. a and b) Experimental and modeled production rates of ^{129}I from Ba for protons with an incident energy of 1600 MeV in gabbro and in iron, respectively. The data are normalized to a proton flux density of 1 cm^{-2} s^{-1}.

Table 4. ^{129}I/^{127}I ratios, ^{129}I atom concentrations, and ^{129}I production rates for four measurements of a Knyahinya sample from 7.5–10.0 cm depth. Production rates are calculated for a 39.4 Myr space exposure (Leya et al. 2000b).

Measurement no.	^{129}I/^{127}I (10^{-12})	^{129}I (10^{9}/kg)	^{129}I (10^{-4} dpm/kg m)	P(^{129}I) (10^{-4} atom min^{-1} [kg m^{-1}]).
1	5.46	3.60	3.02	3.66
2	4.59	3.02	2.53	3.07
3	4.85	3.19	2.68	3.25
4	4.78	3.15	2.64	3.20
Average	4.92 ± 0.37	3.25 ± 0.25	2.72 ± 0.21	3.30 ± 0.25

Table 5a. Te and Ba concentrations obtained for three silicate and one magnetic sample of Knyahinya.

Sample	Te (µg/kg)	Ba (µg/kg)
Silicate 1	508	6386
Silicate 2	492	6436
Silicate 3	564	6228
Magnetic phase	660	3735

Table 5b. Te and Ba concentrations of Knyahinya bulk compared to literature data for L chondrites.

Reference	Sample	Te (µg/kg)	Ba (µg/kg)
This study	Knyahinya bulk	526 ± 38	6260 ± 190
Wasson and Kallemeyn (1988)	L chondrites	480	3700
Walsh and Lipschutz (1982)	Knyahinya (L5)	339	–
Walsh and Lipschutz (1982)	Tadjera (L5)	507	–
Walsh and Lipschutz (1982)	Bruderheim (L6)	331	–

kg for EH chondrites given by Wasson and Kallemeyn (1988).

MODELING THE PRODUCTION OF ^{129}I FROM Te IN METEOROIDS

Production rates were calculated using the model described in detail by Leya et al. (2000b). The production rates were calculated by folding the differential particle spectra of primary and secondary particles with the excitation functions of the relevant nuclear reactions and integrating this expression over the energy range of interest. To compare the modeled production rates with measured data in meteorites, the integral number of GCR particles in the meteoroid orbits has to be known. In a recent paper, Leya et al. (2000b) argued that the measured data in meteorites can best be described with a GCR flux density of 4.06 cm^{-2} s^{-1}. We will use this result for comparison of our modeled

production rates with experimental results. However, for reasons not yet well-understood, the GCR flux density that best describes production rates for thermal and epithermal neutron capture reactions is 2.36 cm^{-2} s^{-1} (Leya et al. 2002) and is only slightly different from the 2.32 cm^{-2} s^{-1} needed to reproduce the measured ^{60}Co data in St. Robert using the same set of modeling calculations (Leya et al. 2001). Consequently, in the Appendix, we give results for the ^{129}I production rates from Te separately for the spallogenic and for the neutron capture contributions, each being normalized to a GCR flux density of 1 cm^{-2} s^{-1}. The difference of the contributions of the neutron-capture reaction for the two different primary (surface) flux densities mentioned increases with the overall flux density in the meteoroid (including and dominated by secondary particles) and with the degree of thermalization of the neutrons. These parameters correspond to the depth and the size of the irradiated body, unless the body is too large to be considered a 4π irradiation geometry. In Figs. 5a and 5b, production rates of ^{129}I from Te in stony meteoroids are shown as a function of size and depth for the spallogenic and neutron capture contributions, each being normalized to a primary GCR flux density of 1 cm^{-2} s^{-1}.

Nishiizumi et al. (1983) determined a production rate of 550 atoms ^{129}I min^{-1} (kg Te^{-1}) for the EH4 chondrite Abee in a sample from 13 cm depth. Goswami (1983) determined the preatmospheric radius of Abee as approximately 30 cm. We calculate 551 atom ^{129}I min^{-1} (kg Te^{-1}) for 13 cm depth in a body of 32 cm radius. The approach that is able to describe ^{41}Ca in lunar rocks (primary flux density of 2.36 cm^{-2} s^{-1} for neutron capture reactions but 4.06 cm^{-2} s^{-1} for spallogenic reactions) would result in a production rate of only 424 atom min^{-1} (kg Te^{-1}). However, we would also caution that the chemical composition of Abee is very different from that of ordinary chondrites, for which the particle spectra used in this model have been calculated. This may be of some importance because ^{129}I is a low energy product and matrix effects are expected. However, we have not observed a matrix effect of 30% for any of the cosmogenic nuclides analyzed so far. We would also note that EH chondrites may have experienced a GCR flux density different from the one for ordinary chondrites due to a possibly different orbit. A second data point, with which to compare our model calculations, is the 840 atom min^{-1} (kg Te^{-1}) determined as a production rate for a sample from Allende at 30 cm depth by Nishiizumi et al. (1983). Assuming 85 cm as the preatmospheric radius for Allende, we calculate a production rate of 1494 atom min^{-1} (kg Te^{-1}) for this sample. If we take the analysis of the Allende sample of Nishiizumi et al. (1983) at face value, our modeling seems to overestimate ^{129}I production from Te in large stony meteoroids at intermediate depths. In this case, if we derive the neutron capture component (Leya et al. 2003), using a primary flux density of 2.36 cm^{-2} s^{-1}, we would obtain 964 atom min^{-1} (kg Te^{-1}).

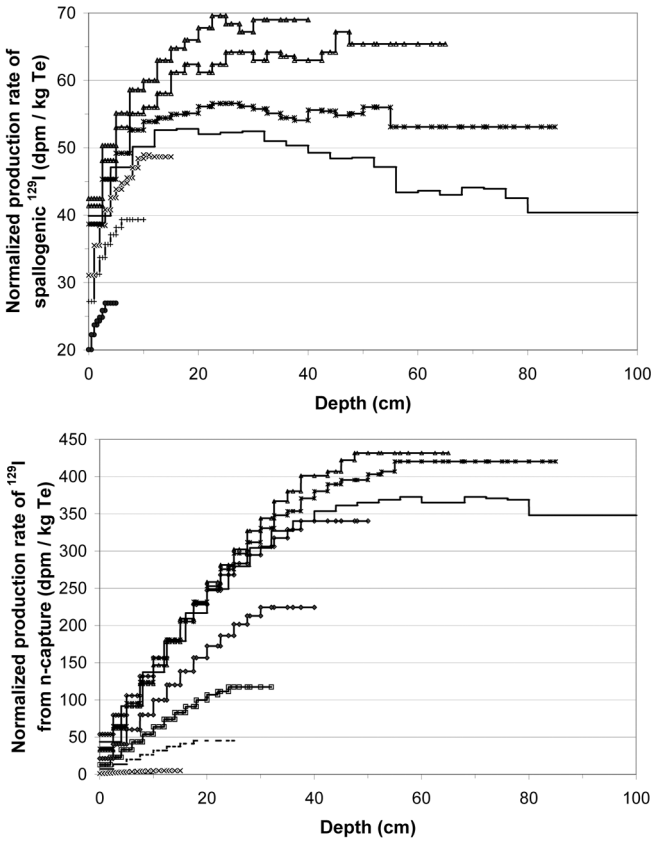

Fig. 5. a and b) Production rates of ^{129}I from Te in stony meteoroids as a function of size and depth normalized to a GCR flux density of 1 cm^{-2} s^{-1}. The contributions of the spallogenic reactions in Fig. 5a and of the neutron capture reaction in Fig. 5b are shown. The modeled radii shown are 5, 10, 15, 40, 65, 85, and 100 cm in Fig. 5a, and in addition to these radii, 25, 32, and 50 cm in Fig. 5b.

MODELING THE PRODUCTION OF ^{129}I FROM Ba IN METEOROIDS

We have calculated normalized production rates of ^{129}I from Ba in stony meteoroids with radii between 5 cm and 100 cm, which are presented in the Appendix.

For a shielding depth of 13 cm in a 32 cm body (Abee sample from Nishiizumi et al. [1983]), we can estimate a production rate of 5.21 atom ^{129}I min^{-1} (kg Ba^{-1}), while for 30 cm shielding depth in a 85 cm meteoroid, the result is 4.49 atom ^{129}I min^{-1} (kg Ba^{-1}).

MODELING THE PRODUCTION OF ^{129}I IN ORDINARY CHONDRITES AND ENSTATITE CHONDRITES

If we assume that only Te and Ba contribute as target elements to the ^{129}I production in meteoroids, and using elemental concentrations from the literature, we can calculate the ^{129}I production rates in meteoroids and compare them to experimental data. We have shown results based on the GCR

flux density derived by Leya et al. (2000b), and these are preliminary because the production by neutron capture needs further investigation.

We will attempt further analysis for the Abee and Allende samples analyzed by Nishiizumi et al. (1983). Using the Te concentration of 2.5 mg/kg used by Nishiizumi et al. (1983) for Abee from Ikramuddin et al. (1976) and 2.8 mg/kg Ba compiled for EH chondrites (Wasson and Kallemeyn 1988), we can calculate a ^{129}I production rate of 1.39×10^{-3} atom ^{129}I min^{-1} (kg m)$^{-1}$ for 13 cm shielding depth (Nishiizumi et al. 1983) in a body of 32 cm radius. This rate is in excellent agreement with the experimental production rate of 1.40×10^{-3} atom ^{129}I min^{-1} (kg m)$^{-1}$ (Nishizumi et al. 1983). When Te and Ba concentrations for EH chondrites are taken from Wasson and Kallemeyn's compilation (1988), i.e., 2.23 mg Te/kg, we obtain 1.24×10^{-3} atom ^{129}I min^{-1} (kg m)$^{-1}$. Using the Te and Ba concentrations determined for Abee in this work, 2.40 mg/kg for the first and 3.15 mg/kg for the latter element, we calculate 1.34×10^{-3} atom ^{129}I min^{-1} (kg m)$^{-1}$.

For the Allende sample analyzed by Nishiizumi et al. (1983), we use the same shielding depth as in that reference, 30 cm, in an 85 cm body. The preliminary modeled production rates, then, is 1.58×10^{-3} atom ^{129}I min^{-1} (kg m)$^{-1}$. For the calculations, Te and Ba concentrations of 1.02 mg/kg and 4.9 mg/kg, respectively (Wasson and Kallemeyn 1988), are used. This result substantially exceeds the experimental result of 9.3×10^{-4} atom ^{129}I min^{-1} (kg m)$^{-1}$ (Nishiizumi et al. 1983). For both samples, we find the contribution of Te to the total ^{129}I production is at least 98%.

For a sample from 7.5–10 cm depth in the 45 cm radius meteorite Knyahinya (Schnabel et al. 2001), using Ba and Te concentrations for L chondrites according to Wasson and Kallemeyn (1988) (3.7 mg/kg Ba and 0.48 mg/kg Te), we obtain 3.39×10^{-4} atom ^{129}I min^{-1} (kg m)$^{-1}$. Our experimental result is 3.30×10^{-4} atom ^{129}I min^{-1} (kg m)$^{-1}$. Using our own experimental elemental concentrations for Knyahinya, 6.26 mg/kg Ba and 0.526 mg/kg Te, we calculate 3.83×10^{-4} atom ^{129}I min^{-1} (kg m)$^{-1}$. Using the average of the Te concentration of the compilation by Wasson and Kallemeyn (1988), our experimental result, 0.503 mg Te/kg m, and the compiled concentration of 3.7 mg/kg m, for Ba, we obtain 3.55×10^{-4} atom min^{-1} (kg m)$^{-1}$.

Previously, we used the ^{129}I analysis in this Knyahinya sample to draw preliminary conclusions about GCR constancy in the past (Schnabel et al. 2001). At that time, we were not aware of the yet unsolved problem of how to treat the neutron capture reaction on ^{128}Te quantitatively. Consequently, we do not make any conclusions about the extent of GCR constancy in the past in this analysis.

Using the very high Ba to Te ratio in H chondrites, 16.2 according to Wasson and Kallemeyn (1988), the relative contribution of Ba to the total ^{129}I production is the highest for this meteorite class. At the surface of 5 cm bodies, Ba gives rise to 39% of the ^{129}I production. In a 25 cm body sample, this value is still as high as 27%. While Te is the most important target element even for H chondrites of all sizes and at all depths, reactions on Ba also contribute substantially to the total ^{129}I production in H chondrites. This is especially true at shallower locations in small bodies, where neutron capture on ^{128}Te is not as important. For L chondrites, with a Ba to Te ratio of 7.7 (Wasson and Kallemeyn 1988), Ba gives rise to 23% of the total ^{129}I production at the surface of a 5 cm body and to 15% of the total production at the surface of a 25 cm body. EH chondrites exhibit a very low Ba to Te concentration ratio of only 1.17 (Wasson and Kallemeyn 1988). Consequently, for this meteorite class, ^{129}I production from Ba is nearly negligible even at the surface of a 5 cm body, where only 4% of the total production is attributed to spallation reactions on Ba.

Further work is needed to improve the model calculations and to answer the question of whether the ^{129}I production by neutron capture is best described by a GCR flux of 4.06 cm^{-2} s^{-1} or by the lower value of 2.36 cm^{-2} s^{-1}.

CONCLUSIONS

We have demonstrated the reproducibility of the radiochemical separation procedures used especially for irradiated Te and Ba-glass samples. For Cu_2Te, the applied procedure always has to be checked by processing at least two aliquots of every sample. The accuracy and reproducibility of the AMS measurements of ^{129}I in Zurich was previously demonstrated by Schnabel et al. (2000).

A novel method for the determination of Te in meteorites has been presented. Elemental production rates of ^{129}I per kg Te can now be calculated based on a reliable chemical analysis without using neutron activation analysis.

In spite of the fact that the determination of the proton-induced excitation function for the production of ^{129}I from Te can be considered almost complete, a second determination of the production cross sections for proton energies below 20 MeV may be desirable. This is because of the importance of that energy range for ^{129}I production and also because of the relatively large standard deviations for the cross sections in this energy range. For the neutron induced excitation function, the situation is much better than for most other cosmogenic nuclides because the cross section has been measured at 14.7 MeV. However, additional data points could be determined between the threshold of the ^{130}Te(n, 2n)$^{129m+g}$Te reaction and 14.7 MeV. The local maxima and minima found for the experimental proton-induced excitation function from Te above 50 MeV are probably experimental artifacts but should not give rise to problems in the modeling of ^{129}I production in meteoroids. We do not expect protons in this energy range to contribute significantly to ^{129}I production.

The experimental data set shown for the proton-induced production from Ba can be considered complete. We can also

confirm the smaller contribution of Ba, compared to Te, as a target element for the production of ^{129}I in meteoroids.

For the modeling of ^{129}I production in meteoroids, our preliminary model calculations agree well with experimental data (Nishiizumi et al. 1983) and this work for two different samples from medium-sized meteoroids, when 4.06 cm^{-2} s^{-1} is used as GCR flux density. Note that by using 4.06 cm^{-2} s^{-1} as the flux density of primary GCR particles, the model is capable of describing experimental ^{10}Be, ^{26}Al, ^{36}Cl, and ^{53}Mn production rates, usually within the experimental uncertainties (Leya et al. 2000b). However, with that flux density, the ^{129}I production in larger bodies such as Allende, i.e., R >65 cm, is calculated to exceed the experimentally determined production (Nishiizumi et al. 1983) substantially. Moreover, our preliminary modeling cannot describe the neutron capture products ^{41}Ca in lunar rocks (Leya et al. 2002) and ^{60}Co in St. Robert (Leya et al. 2001). In conclusion, the contribution of the neutron capture reaction on ^{128}Te to the ^{129}I production in meteoroids needs further investigation.

Acknowledgments–This work was supported by the German National Science Foundation (DFG), Bonn (Grant No. Schn 507/1) and by the Swiss National Science Foundation (SNF), Berne. The authors are grateful to S. M. Qaim and A. Hohn for advice and support during the irradiation with protons below 20 MeV at the Compact Cyclotron CV28 of the Forschungszentrum Jülich. Moreover, the skill and the assistance of the accelerator staff at T. Svedberg Laboratory in Uppsala and at LNS (Saclay) are greatly appreciated. We thank R. K. Herd (Geological Survey of Canada) for making the Abee sample available for chemical analysis and G. F. Herzog for discussions about the analysis of Knyahinya. The authors are grateful to R. Wieler for making the Knyahinya sample available for ^{129}I and chemical analysis as well as for discussions. We appreciate that the AC laboratory in Spiez, Switzerland made the ICP-MS measurements of the meteorite samples possible. Technical assistance by E. Vogel (University of Bern) is gratefully acknowledged. The authors are grateful for the comments and suggestions of K. Nishiizumi in his review of this manuscript. E. Zinner and T. Jull improved this manuscript.

Editorial Handling—Dr. Ernst Zinner

REFERENCES

Binz C. M., Kurimoto R. K., and Lipschutz M. E. 1974. Trace elements in primitive meteorites: V. Abundance patterns of thirteen trace elements and interelement relationships in enstatite chondrites. *Geochimica et Cosmochimica Acta* 38:1579–1606.

Blann M. 1972. Hybrid model for pre-equilibrium decay in nuclear reactions. *Physical Review Letters* 27:337–340.

Elmore D., Gove H. E., Ferraro R., Kilius L. R., Lee H. W., Chang K. H., Beukens R. P., Litherland A. E., Russo C. J., Purser K. H., Murrell M. T., and Finkel R. C. 1980. Determination of ^{129}I using tandem accelerator mass spectrometry. *Nature* 286:138–140.

Goswami J. N. Nuclear track records in the Abee enstatite chondrite 1983. *Earth and Planetary Science Letters* 62:159–164.

Graf T. 1988. Produktion kosmogener Nuklide in Meteoriten. Ph.D. thesis, ETH Zürich, Switzerland.

Hertogen J., Janssens M. J., Takahashi A., Morgan J. W., and Anders E. 1983. Enstatite chondrites: Trace element clues to their origin. *Geochimica et Cosmochimica Acta* 47:2241–2255.

Hohn A., Coenen H. H., and Qaim S. M. 1998a. Nuclear data relevant to the production of ^{120g}I via the ^{120}Te(p, n) process at a small-sized cyclotron. *Applied Radiation and Isotopes* 49:1493–1496.

Hohn A., Scholten B., Coenen H. H., and Qaim S. M. 1998b. Excitation functions of (p, xn) reactions on highly enriched ^{122}Te: Relevance to the production of ^{120g}I. *Applied Radiation and Isotopes* 49:93–98.

Hohn A., Nortier F. M., Scholten B., Van der Walt T. N., Coenen H. H., and Qaim S. M. 2001. Excitation functions of ^{125}Te(p, xn) reactions from their respective thresholds up to 100 MeV with special reference to the production of ^{124}I. *Applied Radiation and Isotopes* 55:149–156.

Ikramuddin M., Binz C. M., and Lipschutz M. E. 1976. Thermal metamorphism of primitive meteorites: II. Ten trace elements in Abee enstatite chondrite heated at 400–1000 °C. *Geochimica et Cosmochimica Acta* 40:133–142.

Joint Evaluated File 2.2 2000. The JEF 2.2 Nuclear data library. JEF Report 17. Paris: The Nuclear Energy Agency.

Krähenbühl U., Morgan J. W., Ganapathy R., and Anders E. 1973. Abundance of 17 trace elements in carbonaceous chondrites. *Geochimica et Cosmochimica Acta* 37:1353–1370.

Lavielle B., Toe S., and Gilabert E. 1997. Noble gas measurements in the L/LL5 chondrite Knyahinya. *Meteoritics & Planetary Science* 32:97–107.

Leya I., Lange H. J., Lüpke M., Neupert U., Daunke R., Fanenbruck O., Michel R., Rösel R., Meltzow B., Schiekel T., Sudbrock F., Herpers U., Filges D., Bonani G., Dittrich-hannen B., Suter M., Kubik P. W., and Synal H. A. 2000a. Simulation of the interaction of galactic cosmic ray protons with meteoroids: On the production of radionuclides in thick gabbro and iron targets irradiated isotropically with 1.6 GeV protons. *Meteoritics & Planetary Science* 35:287–318.

Leya I., Lange H. J., Neumann S., Wieler R., and Michel R. 2000b. The production of cosmogenic nuclides in stony meteoroids by galactic cosmic ray particles. *Meteoritics & Planetary Science* 35:259–286.

Leya I., Wieler R., Aggrey K., Herzog G. F., Schnabel C., Metzler K., Hildebrand A. R., Bouchard M., Jull A. J. T., Andrews H. R., Wang M. S., Ferko T. E., Lipschutz M. E., Wacker J. F., Neumann S., and Michel R. 2001. Exposure history of the St. Robert (H5) fall. *Meteoritics & Planetary Science* 36:1479–1494.

Leya I., Wieler R., and Halliday A. N. 2003. The influence of cosmic ray production on extinct nuclide systems. *Geochimica et Cosmochimica Acta* 67:529–541.

Lopez-Gutierrez J. M., Synal H. A., Suter M., Schnabel C. H., Garcia-Leon M. 2000. Accelerator mass spectrometry as a powerful tool for the determination of ^{129}I in rainwater. *Applied Radiation and Isotopes* 53:81–85.

Nishiizumi K., Elmore D., Honda M., Arnold J. R., and Gove H. E. 1983. Measurements of ^{129}I in meteorites and lunar rock by tandem accelerator mass spectrometry. *Nature* 305:611–612.

Nishiizumi K., Arnold J. R., Elmore D., and Kubik P. W. 1985. Cosmogenic ^{129}I in iron meteorites. *Meteoritics* 20:719–720.

Nishiizumi K., Kubik P. W., Sharma P., and Arnold J. R. 1989. ^{129}I depth profiles in cores from Jilin and the Moon. *Meteoritics* 24:310.

Nishiizumi K., Arnold J. R., and Sharma P. 1993. Two-stage exposure of the Fayetteville meteorite based on ^{129}I. *Meteoritics* 28:412–413.

Piel H., Qaim S. M., and Stöcklin G. 1992. Excitation functions of (p, xn) reactions on natNi and highly enriched ^{62}Ni: Possibility of production of medically important radioisotope ^{62}Cu at a small cyclotron. *Radiochimica Acta* 57:1–5.

Schnabel C., Gartenmann P., Lopez-Gutierrez J. M., Dittrich-Hannen B., Suter M., Synal H. A., Leya I., Gloris M., Michel R., Sudbrock F., and Herpers U. 1997. Determination of proton-induced production cross sections and production rates of ^{129}I and ^{41}Ca. In *Proceedings of the Italian physical society 59, Nuclear data for science and technology,* edited by Reffo G. et al. Bologna: Società Italiana di Fisica. pp. 1559–1561.

Schnabel C., Leya I., Michel R., Csikai J., Dezso Z., Lopez-Gutierrez J. M., and Synal H. A. 2000. Non-destructive and radiochemical determination of the neutron-induced production cross section of I-129 from Te and other neutron-induced cross sections on Te at 14.7 MeV. *Radiochimica Acta* 88:439–443.

Schnabel C., Leya I., Wieler R., Herd R. K., Synal H. A., Krähenbühl U., and Herzog G. F. 2001. ^{129}I in Knyahinya and Abee and a first estimate of GCR constancy over 20 Myr (abstract). *Meteoritics & Planetary Science* 36:A183–A184.

Scholten B., Kovacs Z., Tarkayi F., and Qaim S. M. 1995. Excitation functions of ^{124}Te(p, xn)$^{124, 123}$I reactions from 6 to 31 MeV with special reference to the production of ^{124}I at a small cyclotron. *Applied Radiation and Isotopes* 46:255–259.

Shubin Y. N., Lunev V. P., Konobeyev A. Y., and Dityuk A. I. 1995. Computer code ALICE-IPPE, IAEA, INDC(CCP)-385, Vienna.

Steyn G. F., Mills S. J., Nortier F. M., Simpson B. R. S., and Meyer B. R. 1990. Production of ^{52}Fe via proton-induced reactions on manganese and nickel. *Applied Radiation and Isotopes* 41:315.

Synal H. A., Bonani G., Döbeli M., Ender R. M., Gartenmann P., Kubik P. W., Schnabel C. H., and Suter M. 1997. Status report of the PSI/ETH AMS facility. *Nuclear Instruments and Methods in Physical Research Section B* 123:62–68.

Takacs S., Tarkanyi F., Sonck M., and Hermanne A. 2002. New cross-sections and intercomparison of proton monitor reactions on Ti, Ni, and Cu. *Nuclear Instruments and Methods in Physical Research Section B* 188:106–111.

Tarkanyi F., Takacs S., Gul K., Hermanne A., Mustafa M. G., Nortier M., Oblozinsky P., Qaim S. M., Scholten B., Shubin Y. N., and Youxiang Z. 2001. Bema monitor reactions. In *Charged particle cross section database for medical radioisotope production: Diagnostic radioisotopes and monitor reactions.* Technical document 1211. Vienna: International Atomic Energy Agency. pp. 49–152.

Tobailem J. and De Lassus St. Genies C. H. 1981. Report CEA-N-1466 (5).

Walsh T. M. and Lipschutz M. E. 1982. Chemical studies of L chondrites: II. Shock-induced trace element mobilization. *Geochimica et Cosmochimica Acta* 46:2491–2500.

Wasson J. T. and Kallemeyn G. W. 1988. Composition of chondrites. *Philosophical Transactions of the Royal Society of London Series A* 325:535–544.

APPENDIX

Table A1. Calculated elemental GCR production rates of ^{129}I formed by spallogenic reactions from Te and by neutron capture on Te as well as by spallogenic reactions from Ba, respectively. All production rates are normalized to an overall primary GCR flux density of 1 cm^{-2} s^{-1}.

Radius (cm)	Depth (d/R)	Spallogenic ^{129}I from Te (atom min^{-1} [kg Te^{-1}])	Neutron-capture ^{129}I from Te (atom min^{-1} [kg Te^{-1}])	Spallogenic ^{129}I from Ba (atom min^{-1} [kg Ba^{-1}])
5	0.00–0.10	20.0	0.18	0.793
5	0.10–0.20	22.3	0.24	0.821
5	0.20–0.30	23.7	0.28	0.836
5	0.30–0.40	24.3	0.31	0.845
5	0.40–0.50	24.8	0.34	0.850
5	0.50–0.60	25.9	0.35	0.876
5	0.60–1.00	26.9	0.38	0.887
10	0.00–0.10	27.2	0.52	0.887
10	0.10–0.20	31.2	0.75	0.923
10	0.20–0.30	33.7	0.94	0.956
10	0.30–0.40	35.7	1.11	0.982
10	0.40–0.50	37.1	1.25	0.992
10	0.50–0.60	38.2	1.38	1.01
10	0.60–1.00	39.3	1.63	1.04
15	0.00–0.07	31.1	1.16	0.931
15	0.07–0.13	35.5	1.67	0.982
15	0.13–0.20	38.5	2.17	1.02
15	0.20–0.27	40.8	2.62	1.04
15	0.27–0.33	42.6	3.10	1.06
15	0.33–0.40	43.9	3.52	1.08
15	0.40–0.47	44.8	3.80	1.08
15	0.47–0.53	45.5	4.11	1.09
15	0.53–0.60	47.0	4.39	1.11
15	0.60–0.67	48.4	4.70	1.11
15	0.67–0.73	49.0	5.02	1.12

Table A1. Calculated elemental GCR production rates of ^{129}I formed by spallogenic reactions from Te and by neutron capture on Te as well as by spallogenic reactions from Ba, respectively. All production rates are normalized to an overall primary GCR flux density of 1 cm^{-2} s^{-1}. *Continued.*

Radius (cm)	Depth (d/R)	Spallogenic ^{129}I from Te (atom min^{-1} [kg Te^{-1}])	Neutron-capture ^{129}I from Te (atom min^{-1} [kg Te^{-1}])	Spallogenic ^{129}I from Ba (atom min^{-1} [kg Ba^{-1}])
15	0.73–1.00	48.7	5.00	1.10
25	0.00–0.10	39.8	7.17	1.03
25	0.10–0.20	47.8	13.5	1.12
25	0.20–0.30	52.6	20.0	1.17
25	0.30–0.40	56.2	26.2	1.22
25	0.40–0.50	59.2	31.9	1.24
25	0.50–0.60	59.9	37.3	1.26
25	0.60–0.70	61.8	41.3	1.28
25	0.70–1.00	62.4	45.3	1.30
32	0.00–0.06	40.3	12.9	1.02
32	0.06–0.13	47.2	23.0	1.11
32	0.13–0.19	51.8	33.1	1.16
32	0.19–0.25	55.2	43.5	1.20
32	0.25–0.31	57.5	54.0	1.23
32	0.31–0.38	59.8	63.9	1.26
32	0.38–0.44	61.5	74.0	1.28
32	0.44–0.50	63.2	82.9	1.31
32	0.50–0.56	64.4	91.1	1.32
32	0.56–0.63	65.8	99.8	1.33
32	0.63–0.69	65.4	107	1.34
32	0.69–0.75	66.3	111	1.35
32	0.75–1.00	66.8	117	1.34
40	0.00–0.06	42.5	21.3	1.04
40	0.06–0.13	50.3	40.5	1.13
40	0.13–0.19	55.1	60.1	1.18
40	0.19–0.25	58.6	79.9	1.21
40	0.25–0.31	60.0	99.8	1.25
40	0.31–0.38	63.0	120	1.28
40	0.38–0.44	64.8	138	1.33
40	0.44–0.50	66.0	157	1.37
40	0.50–0.56	67.8	173	1.38
40	0.56–0.63	69.6	186	1.39
40	0.63–0.69	68.4	202	1.39
40	0.69–0.75	67.2	213	1.40
40	0.75–1.00	69.0	224	1.45
50	0.00–0.05	42.0	53.8	0.990
50	0.05–0.10	50.0	79.5	1.10
50	0.10–0.15	54.4	106	1.18
50	0.15–0.20	57.9	132	1.22
50	0.20–0.25	60.3	157	1.23
50	0.25–0.30	62.1	181	1.25
50	0.30–0.35	63.5	205	1.28
50	0.35–0.40	65.0	228	1.29
50	0.40–0.45	66.9	247	1.30
50	0.45–0.50	67.7	268	1.32
50	0.50–0.55	67.0	283	1.31
50	0.55–0.60	68.2	295	1.31
50	0.60–0.65	67.5	306	1.31
50	0.65–0.70	68.1	318	1.32
50	0.70–0.75	67.1	329	1.31
50	0.75–0.80	65.5	340	1.35
50	0.80–1.00	66.4	340	1.33
65	0.00–0.04	41.4	32.5	0.965

Table A1. Calculated elemental GCR production rates of ^{129}I formed by spallogenic reactions from Te and by neutron capture on Te as well as by spallogenic reactions from Ba, respectively. All production rates are normalized to an overall primary GCR flux density of 1 cm^{-2} s^{-1}. *Continued.*

Radius (cm)	Depth (d/R)	Spallogenic ^{129}I from Te (atom min^{-1} [kg Te^{-1}])	Neutron-capture ^{129}I from Te (atom min^{-1} [kg Te^{-1}])	Spallogenic ^{129}I from Ba (atom min^{-1} [kg Ba^{-1}])
65	0.04–0.08	48.1	61.8	1.06
65	0.08–0.12	53.0	91.5	1.10
65	0.12–0.15	55.1	122	1.15
65	0.15–0.19	56.0	147	1.17
65	0.19–0.23	58.1	178	1.21
65	0.23–0.27	61.2	209	1.21
65	0.27–0.31	62.4	230	1.22
65	0.31–0.35	61.2	259	1.24
65	0.35–0.39	62.4	281	1.25
65	0.39–0.42	64.2	302	1.26
65	0.42–0.46	64.2	327	1.25
65	0.46–0.50	63.0	344	1.24
65	0.50–0.54	64.2	367	1.26
65	0.54–0.58	63.6	380	1.26
65	0.58–0.62	63.0	401	1.28
65	0.62–0.65	63.0	401	1.25
65	0.65–0.69	64.2	407	1.25
65	0.69–0.73	67.2	422	1.28
65	0.73–1.00	65.4	432	1.22
85	0.00–0.03	38.7	34.4	0.892
85	0.03–0.06	45.3	64.6	0.977
85	0.06–0.09	49.2	95.8	1.01
85	0.09–0.12	52.6	124	1.06
85	0.12–0.15	53.9	156	1.08
85	0.15–0.18	54.4	181	1.09
85	0.18–0.21	55.0	205	1.11
85	0.21–0.24	55.1	232	1.12
85	0.24–0.27	56.1	253	1.10
85	0.27–0.29	56.6	276	1.11
85	0.29–0.32	56.6	297	1.11
85	0.32–0.35	56.2	312	1.11
85	0.35–0.38	55.8	331	1.10
85	0.38–0.41	55.1	348	1.10
85	0.41–0.44	54.5	354	1.09
85	0.44–0.47	54.1	371	1.11
85	0.47–0.50	55.6	380	1.10
85	0.50–0.53	55.5	390	1.09
85	0.53–0.56	54.8	396	1.08
85	0.56–0.59	55.1	396	1.10
85	0.59–0.62	56.1	403	1.07
85	0.62–0.65	56.0	407	1.05
85	0.65–1.00	53.1	420	1.06
100	0.00–0.04	39.9	43.7	0.883
100	0.04–0.08	47.1	91.8	0.973
100	0.08–0.12	50.2	137	1.02
100	0.12–0.16	52.6	179	1.05
100	0.16–0.20	52.8	217	1.04
100	0.20–0.24	52.0	249	1.02
100	0.24–0.28	52.3	280	1.01
100	0.28–0.32	52.4	304	0.996
100	0.32–0.36	51.0	327	1.01
100	0.36–0.40	50.3	340	1.01
100	0.40–0.44	49.3	354	0.973

Table A1. Calculated elemental GCR production rates of ^{129}I formed by spallogenic reactions from Te and by neutron capture on Te as well as by spallogenic reactions from Ba, respectively. All production rates are normalized to an overall primary GCR flux density of 1 cm^{-2} s^{-1}. *Continued.*

Radius (cm)	Depth (d/R)	Spallogenic ^{129}I from Te (atom min^{-1} [kg Te^{-1}])	Neutron-capture ^{129}I from Te (atom min^{-1} [kg Te^{-1}])	Spallogenic ^{129}I from Ba (atom min^{-1} [kg Ba^{-1}])
100	0.44–0.48	48.4	361	0.943
100	0.48–0.52	48.5	365	0.915
100	0.52–0.56	47.2	369	0.902
100	0.56–0.60	43.4	373	0.912
100	0.60–0.64	43.6	365	0.878
100	0.64–0.68	43.0	365	0.903
100	0.68–0.72	44.1	373	0.872
100	0.72–0.76	43.9	371	0.893
100	0.76–0.80	42.5	369	0.806
100	0.80–1.00	40.4	348	0.821